



# Replication of laser dynamics using reservoir computing

Atsuya Kawakami<sup>1,\*</sup>, Kazutaka Kanno<sup>1</sup> and Atsushi Uchida<sup>1,\*\*</sup>

<sup>1</sup>Department of Information and Computer Sciences, Saitama University,  
255 Shimo-okubo, Sakura-ku, Saitama City, Saitama 338-8570, Japan

Email: \*a.kawakami.584@ms.saitama-u.ac.jp, \*\*auchida@mail.saitama-u.ac.jp

**Abstract**– We use reservoir computing to replicate the long-term dynamics of a chaotic semiconductor laser with optical feedback. The real and imaginary parts of the electric-field amplitude are used as an input signal for reservoir computing. The attractor of the real and imaginary parts is successfully replicated with high accuracy using reservoir computing.

## 1. Introduction

Neural networks have been actively studied in recent years. Neural networks are information processing technologies that mimic the human brain, and used for various information processing such as image classification. Neural networks with mutual coupling between nodes and self-feedback are called recurrent neural networks, and are suitable for time-dependent data processing such as speech recognition. While recurrent neural networks have high information processing capabilities, they have a disadvantage that the learning algorithm is complex and computationally expensive because all weights of the connections must be learned.

Reservoir computing is a concept derived from recurrent neural networks [1]. Unlike recurrent neural networks, the input weights and network weights among the nodes are fixed randomly, and only the output weights are optimized by learning, which reduces the computational complexity in learning. Physical implementation of reservoir computing has also been reported, because it is easy to implement reservoir computing using a single nonlinear element of a physical device [2-6].

One of the applications using reservoir computing is the replication of nonlinear dynamics [7-9]. It is possible to reproduce the dynamics of a target model by learning only from time series data using reservoir computing. Replication of various nonlinear dynamical models has been reported, and replication of more complex models is needed. One of the nonlinear dynamical models is a semiconductor laser with optical feedback [10]. The dynamics of this model is characterized by high dimensionality of complex electric-field amplitude due to the existence of time-delayed feedback, which results in

multiple positive Lyapunov exponents. Replication of such a complex dynamics of the semiconductor laser optical feedback has not been reported yet using reservoir computing.

In this study, we replicate the dynamics of a semiconductor laser with optical feedback using reservoir computing. The replication is performed using the temporal waveforms of the electric-field amplitude of the target laser dynamics. The similarity of the replicated temporal waveforms to the original waveforms are evaluated by comparing FFT and autocorrelation function.

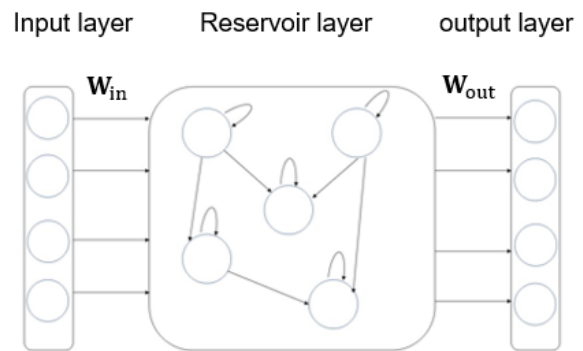


Fig. 1 Schematic diagram of reservoir computing using echo state network.

## 2. Reservoir computing using echo state network

Figure 1 shows a schematic diagram of reservoir computing using echo state network. Reservoir computing consists of an input layer, a reservoir layer, and an output layer. The input signal is sent from the input layer to the reservoir layer using a randomly fixed input weight matrix  $\mathbf{W}_{in}$ . The nodes in the reservoir layer are connected by randomly fixed coupling weight matrix  $\mathbf{W}_{res}$ . In the reservoir layer, a nonlinear transformation is performed to update the node state vector  $\mathbf{r}(t)$  through a high-dimensional mapping. The formula of the node state is described as follows.

$$\mathbf{r}(t + \Delta t) = \alpha \mathbf{r}(t) + \beta f(\mathbf{W}_{res} \mathbf{r}(t) + \mathbf{W}_{in} \mathbf{u}(t) + \mathbf{W}_b) \quad (1)$$

where  $\mathbf{u}(t)$  is the input vector and  $\mathbf{W}_b$  is the random bias matrix, where  $\mathbf{W}_b$  consists of uniform random numbers in

ORCID iDs

Atsuya Kawakami: 0000-0002-2662-0342,

Kazutaka Kanno: 0000-0002-2982-4308

Atsushi Uchida: 0000-0002-4654-8616



This work is licensed under a Creative Commons  
Attribution-NonCommercial-NoDerivatives 4.0 International.

the range  $[-1,1]$ .  $\alpha$  is the leakage rate and  $\beta$  is the input gain. By changing the parameter values of  $\alpha$  and  $\beta$ , the influence from the previous state can be varied.  $f(\cdot)$  is a nonlinear function, where  $\tanh(\cdot)$  is used in this study. In the output layer, the output is obtained by calculating a weighted linear sum of the nonlinear node states and the output weight matrix  $\mathbf{W}_{\text{out}}$  that are optimized by learning. The expression of the output  $\mathbf{y}(n)$  is described as follows.

$$\mathbf{y}(n) = \mathbf{W}_{\text{out}}\mathbf{r}(t) \quad (2)$$

$\mathbf{W}_{\text{out}}$  is optimized by the least-squares method. The formula of the optimization of  $\mathbf{W}_{\text{out}}$  is described as follows.

$$\mathbf{W}_{\text{out}} = \mathbf{D}\mathbf{X}^T(\mathbf{X}\mathbf{X}^T + \lambda\mathbf{I}) \quad (3)$$

where  $\mathbf{D}$  is the target matrix, and  $\mathbf{X}$  is the matrix obtained from the node states.  $\mathbf{I}$  is the identity matrix, and  $\lambda$  is the ridge parameter. The addition of the ridge parameter suppresses over-training.

### 3. Laser dynamics of target signal

The dynamics of a semiconductor laser with optical feedback is numerically calculated as a target signal for the replication of nonlinear dynamics using reservoir computing. The Lang - Kobayashi equation is used as the numerical model [10]. The Lang - Kobayashi equation is described as follows.

$$\frac{dE_{re}(t)}{dt} = \frac{1}{2} \left[ \frac{G_N(N(t) - N_0)}{1 + \epsilon(E_{re}^2(t) + E_{im}^2(t))} \right] [E_{re}(t) - \alpha E_{im}(t)] + \kappa [E_{re}(t - \tau) \cos(\omega\tau) + E_{im}(t - \tau) \sin(\omega\tau)] \quad (4)$$

$$\frac{dE_{im}(t)}{dt} = \frac{1}{2} \left[ \frac{G_N(N(t) - N_0)}{1 + \epsilon(E_{re}^2(t) + E_{im}^2(t))} \right] [\alpha E_{re}(t) + E_{im}(t)] + \kappa [-E_{re}(t - \tau) \sin(\omega\tau) + E_{im}(t - \tau) \cos(\omega\tau)] \quad (5)$$

$$\frac{dN(t)}{dt} = J - \frac{N(t)}{\tau_s} - \frac{G_N(N(t) - N_0) (E_{re}^2(t) + E_{im}^2(t))}{1 + \epsilon(E_{re}^2(t) + E_{im}^2(t))} \quad (6)$$

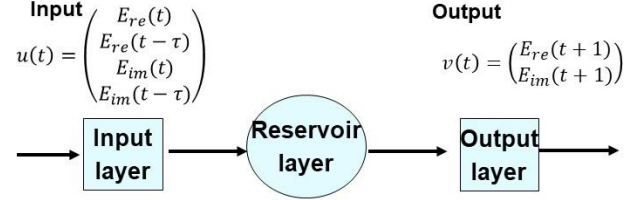
where  $E_{re}(t)$  is the real part of the complex electric field,  $E_{im}(t)$  is the imaginary part of the complex electric field, and  $N(t)$  is the carrier density. The dynamics of the laser intensity  $I(t)$  can be calculated by adding the squares of the real and imaginary parts, i.e.,  $I(t) = E_{re}^2(t) + E_{im}^2(t)$ .  $\tau$  is the delay time and it is set to 5 ns.

Chaotic temporal waveforms of the laser intensity can be obtained by simulating Eqs.(4)-(6). The obtained temporal waveforms are sampled at the sampling interval is 0.01 ns. The average period of the chaotic temporal waveforms is 0.65 ns, which is approximately 65 points per period. This temporal waveform is normalized by the mean of 0 and three times the standard deviation. The normalization formula is described as follows.

$$x(t) = \frac{I(t) - \mu}{3\sigma} \quad (7)$$

where  $\mu$  is the mean of the chaotic temporal waveform and  $\sigma$  is the standard deviation of the chaotic temporal waveform. We replicate the dynamics of the normalized chaotic temporal waveform using reservoir computing.

#### (a) Training phase



#### (b) Prediction phase

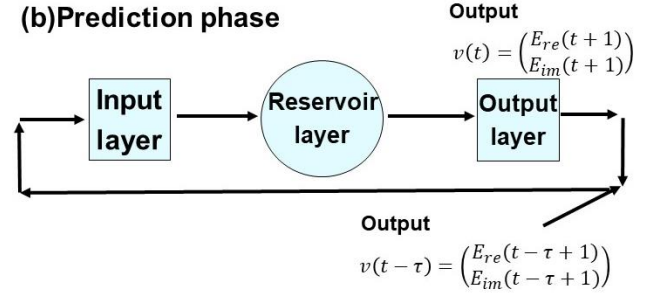


Fig. 2 Prediction scheme. (a) Open-loop configuration for training phase and (b) closed-loop configuration for prediction phase.

### 4. Replication method

Figure 2 shows the schematic diagram of our replication scheme for nonlinear dynamics using reservoir computing. In Fig. 2(a), the output weights are trained so that the output signal is close to the target signal, which is the one-point-ahead input signal. In Fig. 2(b), the output obtained from the reservoir is fed back to the input part to operate autonomously. In this way, reservoir computing can reproduce the trained temporal dynamics.

### 5. Replication results

We replicate the laser dynamics calculated from the Lang -Kobayashi equations using reservoir computing. The input signal is the temporal waveforms of the laser intensity. The reservoir parameters are set to  $\alpha = 0$  and  $\beta = 1$  with 100000 training points and 5000 nodes for the echo state network. The input vector of reservoir computing consists of the real and imaginary parts of the complex electric-field amplitude ( $E_{re}(t)$  and  $E_{im}(t)$ ), and their time-delayed signals shifted by the delay time  $\tau$  ( $E_{re}(t - \tau)$  and  $E_{im}(t - \tau)$ ).

We include the time-delayed signals in the input signal because small correlation of the chaotic temporal waveforms exists at the delay time  $\tau$ . It is important to add the delay information to the input, because the laser

dynamics is determined by the current state and the state before the delay time.

The laser intensity is calculated from the sum of the squares of the real and imaginary parts. However, the real and imaginary parts contain both the intensity and phase information, it is expected that both the laser intensity and phase can be replicated by using reservoir computing.

The feedback signal from the reservoir output in Fig. 2(b) consists of the one-point-ahead signals of the real and imaginary parts ( $E_{re}(t+1)$  and  $E_{im}(t+1)$ ), and their time-delayed outputs ( $E_{re}(t-\tau+1)$  and  $E_{im}(t-\tau+1)$ ).

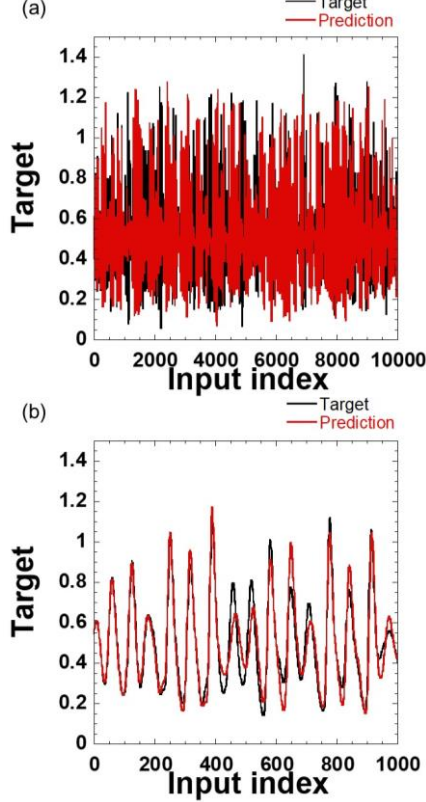


Fig. 3 Result of replication of laser intensity. (a) Replication result. (black) target signal, and (red) prediction signal. (b) Enlarged view of (a).

Figure 3 shows the replication results. The black line in Fig. 3(a) shows the target signal of the laser intensity, and the red line shows the replicated temporal waveform by using reservoir computing. The two temporal waveforms are not matched well. Figure 3(b) shows the enlarged view of Fig. 3(a). In Fig. 3(b), the replicated temporal waveform is close to the target waveform for a short period of time.

The lack of long-term prediction is due to the sensitive dependence of initial conditions of chaos, where the small error can significantly change the long-term behavior. However, the long-term statistical characteristics of the replicated temporal waveforms seems similar to the original dynamics, as shown in Fig. 3(a), even though the temporal waveforms are not matched perfectly. This is

because reservoir computing can learn the characteristics of the laser dynamics.

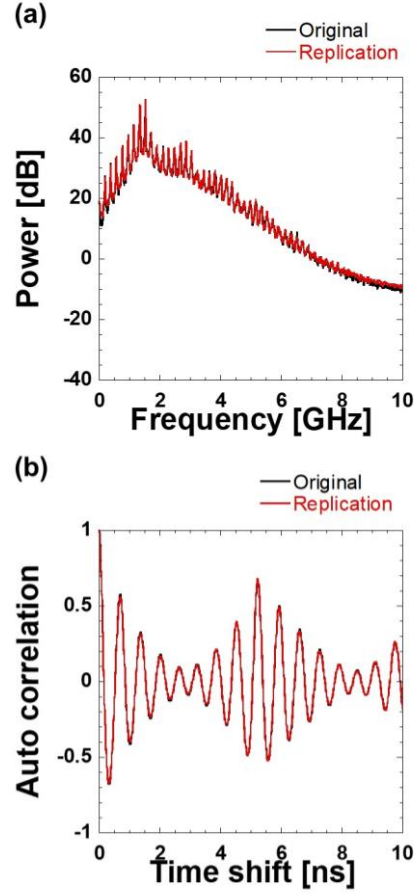


Fig. 4 (a) Fast Fourier transforms (FFT) and (b) autocorrelation functions of (black) target signal and (red) replicated signal.

To evaluate the statistical characteristics of replicated temporal waveforms, we calculate fast Fourier transform (FFT) and autocorrelation function of the temporal waveforms. Figure 4(a) shows the FFTs of the target and replicated temporal waveforms. The two FFTs look very similar and the peaks of the FFTs are matched well. We calculate the correlation value of the two FFTs. The correlation value is 0.9993 and high correlation is obtained.

Figure 4(b) shows the autocorrelation function of the original and replicated temporal waveforms. The two autocorrelation function overlaps very well. We also calculate the correlation value of the two curves. The correlation value is 0.9996, and very high correlation is obtained.

Figure 5 shows the chaotic attractors of the original and replicated dynamics. The chaotic attractors are reconstructed by using  $I(t)$  and  $I(t-\tau)$ . The original and replicated attractors look very similar.

We calculate the Kullback-Leibler divergence as a statistical evaluation of the similarity of the original and replicated attractors. The calculation equation is described as follows.

$$D_{KL}(P||Q) = \sum_i P(i) \log \frac{P(i)}{Q(i)} \quad (8)$$

where  $P(i)$  is the probability distribution of the replicated attractor and  $Q(i)$  is the probability distribution of the original attractor. Smaller Kullback-Leibler divergence indicates more similar attractors. The Kullback-Leibler divergence is calculated from Fig. 5 and the value of 0.01558 is obtained. This result indicates that very similar attractors are obtained, and we succeed in replicating the complex laser dynamics by reservoir computing.

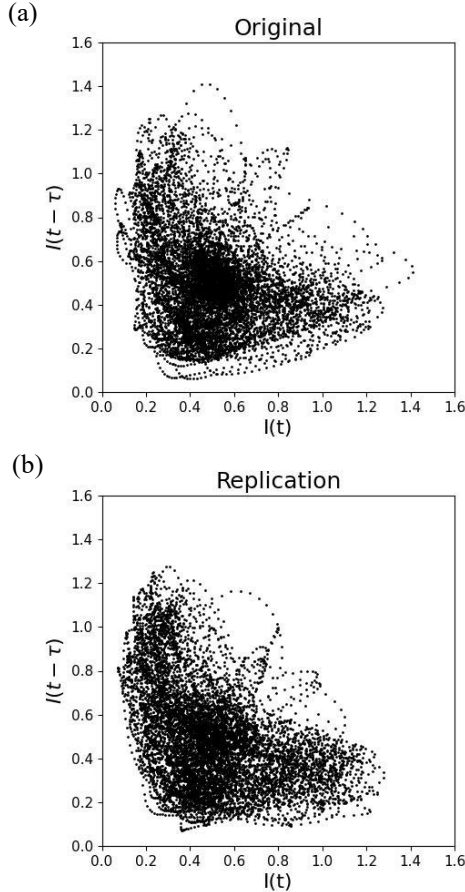


Fig. 5 (a) Original and (b) replicated attractors for laser intensity in the time-delayed phase space.

In our scheme, we use four input signals for training, which are the real and imaginary parts of the complex electric field ( $E_{re}(t)$  and  $E_{im}(t)$ ), and their time-delayed signals ( $E_{re}(t - \tau)$  and  $E_{im}(t - \tau)$ ). The use of these input signals is essential to replicate complete laser dynamics, because both the intensity and phase dynamics can be calculated from these variables. In addition, the inclusion of time-delayed signals is also important to replicate the dynamics of time-delayed systems.

## 6. Conclusions

We replicated the dynamics of laser intensity of a semiconductor laser with optical feedback using reservoir computing with echo state network. The Lang-Kobayashi

equations were used to generate a target signal of the chaotic laser dynamics. The real and imaginary parts of the complex electric-field amplitude of the laser output were used as an input signal to the reservoir, as well as their time-delayed signals. We performed short-term prediction of the chaotic temporal waveforms. We also succeeded in replicating the long-term dynamics of temporal waveforms by using reservoir computing, and the FFT, autocorrelation function and chaotic attractor are well reproduced. Our method can be applied to real experimental data for the replication of long-term nonlinear dynamics.

## Acknowledgments

This study was supported in part by JSPS KAKENHI (JP19H00868, JP20K15185, JP22H05195), JST CREST (JPMJCR17N2), and the Telecommunications Advancement Foundation.

## References

- [1] H. Jaeger, "The "echo state" approach to analysing and training recurrent neural networks – with an Erratum note," German National Research Center for Information Technology GMD Technical Report, Vol. 148, No. 34, pp. 1–13 (2001).
- [2] L. Appeltant, M. C. Soriano, G. Van der Sande, J. Danckaert, S. Massar, J. Dambre, B. Schrauwen, C.R. Mirasso and I. Fischer, "Information processing using a single dynamical node as complex system," Nature Communication, Vol. 2, Article No. 468 (2011).
- [3] I. Estébanez, I. Fischer and M. C. Soriano, "Constructive role of noise for high-quality replication of chaotic attractor dynamics using a hardware-based reservoir computer," Physical Review Applied, Vol. 12, pp. 034058 (2019).
- [4] M. Rafayelyan, J. Dong, Y. Tan, F. Krzakala and S. Gigan, "Large-scale optical reservoir computing for spatiotemporal chaotic systems prediction," Physical Review X, Vol. 10, pp. 041037 (2020).
- [5] D. Brunner, M.C. Soriano, Claudio, R. Mirasso and I Fischer, "Parallel photonic information processing at gigabyte per second data rates using transient states," Nature Communications, Vol. 4, Article No. 1364 (2013).
- [6] K. Kanno, A. A. Haya and A. Uchida, "Reservoir computing based on external-cavity semiconductor laser with optical feedback modulation," Optics Express, Vol. 30, No. 19, pp. 34218-34238 (2022).
- [7] J. Pathak, B. Hunt, M. Girvan, Z. Lu and E. Ott, "Model-free prediction of large spatiotemporally chaotic systems from data: A reservoir computing approach," Physical Review Letters, Vol. 120, pp. 024102 (2018).
- [8] D. J. Gauthier, E. Bollt, A. Griffith and W. A. S. Barbosa, "Next generation reservoir computing," Nature Communication, Vol. 12, pp. 5564 (2021).
- [9] A. Röhm, D. J. Gauthier and I. Fischer, "Model-free inference of unseen attractors: Reconstructing phase space features from a single noisy trajectory using reservoir computing," Chaos, Vol. 31, pp. 103127 (2021).
- [10] R. Lang and K. Kobayashi, "External optical feedback effects on semiconductor injection laser properties," IEEE Journal of Quantum Electronics, Vol. 16, No. 3, pp. 347-355 (1980).